Journal of the Physical Society of Japan
Vol. 69, No. 11, November, 2000, pp. 3656-3659

Magnetoresistance of Lateral Hyperlattice: Independent Control of Spacing and Phase of Commensurability Oscillation

Akira ENDO* and Yasuhiro IYE**

Institute for Solid State Physics, University of Tokyo

(Received June 7, 2000)

Unidirectional lateral lattice of a unit which in itself consists of small number of lateral-superlattice units has been fabricated from two-dimensional electron gas (2DEG) and its magnetoresistance has been measured. It shows commensurability oscillation similar to that of ordinary lateral superlattice (LSL), but with much altered amplitude distribution; the amplitude vanishes at some index n, then increases and decreases with n, in marked contrast to monotonic decrease for ordinary LSL. The amplitude distribution is well explained by the relative abundance of semi-classical trajectories responsible for the corresponding oscillation. The spacing between peaks or dips is determined by the lattice period within a unit, as is the case with commensurability oscillation of ordinary LSL. The phase, on the other hand, is shown to be controlled by the distance between adjacent units, allowing independent manipulation of the spacing and the phase of the magnetoresistance oscillation.

KEYWORDS: 2DEG, lateral superlattice, magnetoresistance oscillation, GaAs, AlGaAs

Lateral superlattice (LSL) — two-dimensional electron gas (2DEG) with additional artificial periodic modulation — is a typical system for studying an interplay between the artificially introduced length, the period a of the superlattice, and characteristic length scales of the electron system itself. Under a magnetic field, B, cyclotron radius $R_c = \hbar k_F/eB$ is one of such characteristic lengths with $k_F = \sqrt{2\pi n_s}$, the Fermi wave number, determined by an important property of 2DEG, the electron density n_s. It is now well established, both experimentally[1)] and theoretically[2-4)] that magnetoresistance (MR) of LSL shows oscillatory behavior resulting from commensurability between R_c and a, provided that mean free path $L = \hbar k_F \mu/e$ of the 2DEG, another characteristic length determined by n_s and the mobility μ, is long enough for the electron to travel the length both R_c and a without being scattered. For periodic electrostatic potential modulation

$$V(x) = V_0 \cos\left(\frac{2\pi}{a}x\right), \tag{1}$$

the oscillation is periodic in $1/B$, and MR trace takes minima at,

$$\frac{2R_c}{a} = n - \frac{1}{4} \quad (n = 1, 2, 3, ...) \tag{2}$$

and maxima at

$$\frac{2R_c}{a} = n - \frac{3}{4} \quad (n = 1, 2, 3, ...) \tag{3}$$

So far, experimental studies of LSL have mainly been confined to devices the potential profile of which can be, at least approximately, described by sinusoid of the form eq. (1). Several papers were concerned with higher harmonics of the potential profile, and reported contribution from second[5,6)] or third[7)] harmonic contents in the MR traces. In the present paper, devices with much more complicated modulation line shape have been studied. As a unit of superlattice, short length superlattice itself, several periods long, has been utilized; p ($3-4$ in the present paper) units of superlattice with period a has been placed alternatively with an empty space of length qa. The overall period is $b = (p+q)a$. Schematic diagram of the sample is given in Fig. 1 along with an SEM image of line-and-space pattern of a device with $p = 3$ and $q = 3$. The devices are, so to speak, superlattice of a lateral superlattice. Therefore it seems appropriate for us to coin a term *lateral hyperlattice*. Unlike ordinary LSL, two length scales, namely the basic period a and the hyperlattice period b, are artificially introduced. The purpose of the present paper is to see the behavior of electrons in such an artificial hyperperiodicity.

Devices are prepared from MBE-grown GaAs/AlGaAs 2DEG with $\mu = 60\,\mathrm{m}^2\ (Vs)^{-1}$ and $n_s = 2.0 \times 10^{15}\,\mathrm{m}^{-2}$, hence $L \approx 5\,\mu$m. The heterointerface resides at $d = 90$ nm below the surface. As mentioned above, L must be much longer than the overall period b. This requires a to be short, since a are designed to be nearly an order of magnitude smaller than b. We adopted $a = 115$ nm in the present study. Two serial Hall bars were prepared on one device. One of them was further processed and the other was reserved as a reference. Potential modulation was introduced by placing on the surface a unidirectional grating of electron-beam (EB) negative resist, and by making use of strain-induced effect. For the resist we used calixarene derivative, which has been developed by NEC group and have shown to have sub 10-nm resolution.[9)] Combined with the use of high-resolution EB machine with field-emission gun (JEOL 6340F), line-patterns $a/2 = 58$-nm wide and about 40-nm high with

* E-mail: akrendo@issp.u-tokyo.ac.jp
** Also at: CREST, Japan Science and Technology Corporation.

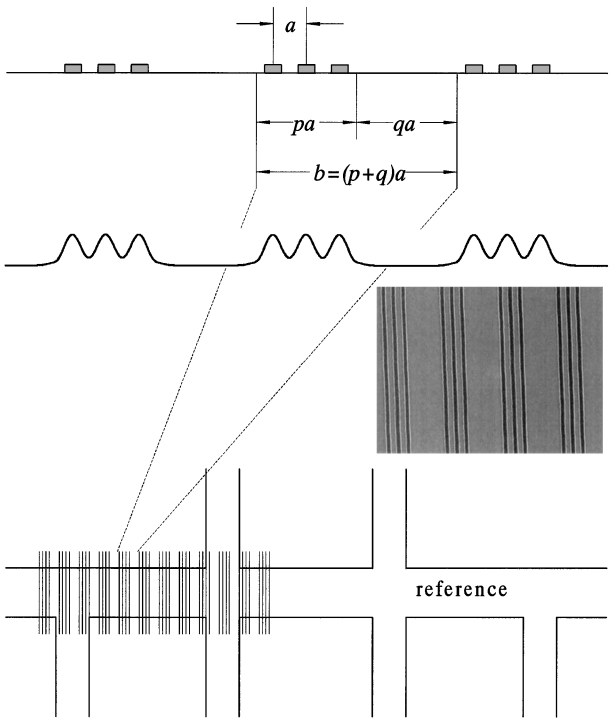

Fig. 1. Schematic diagram of a device, giving the definition of basic period a and hyperlattice period $b = (p + q)a$, along with the potential profile at the 2DEG plane.[8] Also shown is an SEM image of the line-and-space pattern; darker vertical lines represent the EB resist and brighter region open space. The case of $p = q = 3$ is shown as an example.

sharp edges, interdigitated with $a/2$ open spaces, can be delineated without difficulties. The grating causes strain due to differential contraction between the resist and GaAs substrate, when cooled from room temperature down to 4.2 K, the temperature at which measurement was carried out. The strain thus introduced couples to 2DEG mainly through the piezoelectric effect and brings about potential modulation. To maximize the effect,[10,11] the $\langle 110 \rangle$ direction of the GaAs substrate was chosen as the direction of the grating (the direction of the current for MR measurement). The modulation amplitude, however, was only 0.04 meV, or about 0.5% of the Fermi energy $E_F = \pi\hbar^2 n_s/m^*$.[14] The amplitude is much smaller than LSL's reported so far with metal grating (even without bias applied on the gate[6,7]), or with stressor,[12] or LSL made by etching off the surface.[13] This is in part due to small strain and/or Fermi energy pinning of the resist we have chosen and also to small a to d ratio; any effects made at the surface diminish as a rapid function of d/a. The small amplitude is quite advantageous for the present purpose because electron areal density n_s is guaranteed not to vary over the device. Especially it is highly desirable that n_s is uniform within a hyperlattice unit, i.e., between the part pa with LSL on top and the part qa with open surface, since otherwise the interpretation of data would become quite complicated. We have verified that our grating do not cause any change in n_s or deterioration in μ by comparing Hall and Shubnikov-de Haas (SdH) measurements with the reference Hall bar.

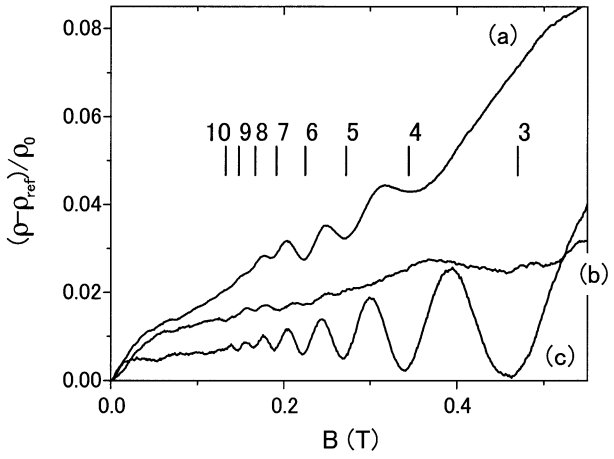

Fig. 2. Magnetoresistance (MR) of devices (a) $p = 3$, $q = 3$, (b) $p = 4$, $q = 4$, and (c) ordinary LSL with period a (or $p = 1$, $q = 0$). Short vertical lines indicate theoretically predicted positions of minima with their indices n, given by eq. (2), for ordinary LSL.

Figure 2 shows magnetoresistance (MR) of samples (a) $p = 3$, $q = 3$, (b) $p = 4$, $q = 4$, and also (c) ordinary LSL with period a (or $p = 1$, $q = 0$) for comparison. In order to eliminate slowly varying background, MR of the adjacent reference Hall bar has been subtracted from each trace shown in the figure. All the samples are prepared from identical wafer and had the same electron density. Short vertical lines in the figure mark the positions of minima theoretically predicted for the ordinary LSL with period a given by eq. (2) along with their indices n. As expected, sample (c) shows minima at the position of eq. (2) from $n = 3$ to 9. For lower indices, i.e., for higher magnetic fields ($B > 0.6$ T), the commensurability oscillation is obscured by the domination of the SdH oscillation. The resistivity minima of (a) occur also at the positions given by eq. (2) for $n = 4$–8 with the structure at $n = 6$ most prominent. A dip at $n = 3$, however, is not discernible. A dip at $n = 9$ also seems to be missing although it is not as clear as for the lower indices because oscillation is weak anyway at low magnetic fields. For (b), $n = 3$ and $n = 5$–8 dips are observed with $n = 8$ most conspicuous and $n = 4$ absent.

Simple explanation of the observed oscillation amplitudes is given by recalling the semiclassical theory of Weiss oscillation.[4] The theory attributes the origin of the oscillation to $\mathbf{E} \times \mathbf{B}$ drift of electrons under modulated electric field $E_x(x) = -[1/(-e)]\mathrm{d}V(x)/\mathrm{d}x$ and $E_y(x) = 0$ ($-e < 0$ denotes the charge of an electron). The drift velocity, $\mathbf{v}_d = (\mathbf{E} \times \mathbf{B})/B^2 = (0, -E_x(x)/B)$, is averaged over one period of cyclotron motion with fixed guiding-center position (X, Y). Then the average $\overline{v_{d,y}}$ is squared and further averaged over X for one lateral period a. (Since the system is one-dimensional, it is treated as uniform in the y direction.) The averaged squared-drift-velocity $\langle \overline{v_{d,y}}^2 \rangle$ is related to the conductivity tensor through Einstein's relation. For the sinusoidal potential modulation of the form eq. (1), the calculation can be completed analytically:

$$\overline{v_{d,y}} = \frac{V_0}{aeB}\int_0^{2\pi} \sin[\frac{2\pi}{a}(X + R_c\cos\phi)]\mathrm{d}\phi$$
$$= \frac{2\pi V_0}{aeB}\sin\left(\frac{2\pi}{a}X\right) J_0\left(\frac{2\pi}{a}R_c\right)$$
$$\approx \frac{2V_0}{eB}\sqrt{\frac{1}{aR_c}}\sin\left(\frac{2\pi}{a}X\right)\cos\left(\frac{2\pi}{a}R_c - \frac{\pi}{4}\right) \quad (4)$$

and

$$\langle\overline{v_{d,y}}^2\rangle = \frac{1}{a}\int_0^a \overline{v_{d,y}}^2\mathrm{d}X$$
$$\approx \left(\frac{V_0}{eB}\right)^2\frac{2}{aR_c}\cos^2\left(\frac{2\pi}{a}R_c - \frac{\pi}{4}\right) \quad (5)$$

The approximation makes use of the asymptotic expression of the 0-th order Bessel function $J_0(2\pi R_c/a)$, valid at large enough R_c/a. The condition for minima (maxima) is equivalent to the condition for $\overline{v_{d,y}}^2$ to take zero (maxima), and reads eq. (2) (eq. (3)). An example of trajectory that gives minima is shown in Fig. 3(a). For large R_c/a, the function to be integrated oscillates rapidly with ϕ in the cyclotron-motion averaging eq. (4). Thus the main contribution to the integral is from the vicinity of stationary points $\phi = 0$ and π, where the velocity is parallel to the y direction; for a cyclotron trajectory with a given R_c, the modulation it experiences at both edges with the largest and smallest x is the most important ingredient for determining its contribution to resistivity. It follows that the contribution is the same, to a good approximation, even if the modulation at the interior of the trajectory is totally absent (Fig. 3(b)).

In the case of $p = q = 3$, cyclotron trajectories of the type shown in Fig. 3(a) are present only for $n = 1$ and 2 minima. Cyclotron trajectories of the type Fig. 3(b) emerge for $n = 4-8$ minima, while both types are inhibited for $n = 3$ and 9. Figure 4 depicts the cyclotron trajectories responsible for minima. Only those with guiding center positions $X = (i/2 + 1/4)a$ with i integers, which give main contribution in guiding center averaging eq. (5), are shown. For $n = 3$ and 9, at least one of the edges of the trajectories (shown as dotted circles) are outside the region, delineated by thin solid lines, of potential modulation and cannot therefore contribute to resistivity minima. For $n = 4$–8, the number of trajectories increases with n, reaches maximum at $n = 6$, and then decreases. The observed oscillation amplitude in Fig. 2(a) can be thought of as reflecting the number of trajectories shown in Fig. 4. The largest dip for $n = 8$

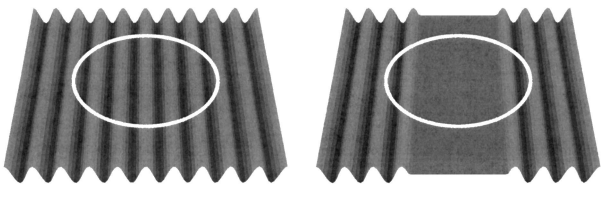

Fig. 3. (a) Sketch of cyclotron trajectory that contributes to n-th minimum in MR for a periodic potential modulation (the case for $n = 6$ is depicted). (b) Cyclotron trajectory that makes approximately the same contribution to MR as (a) for a modified potential modulation. Three periods are omitted from the periodic modulation of (a).

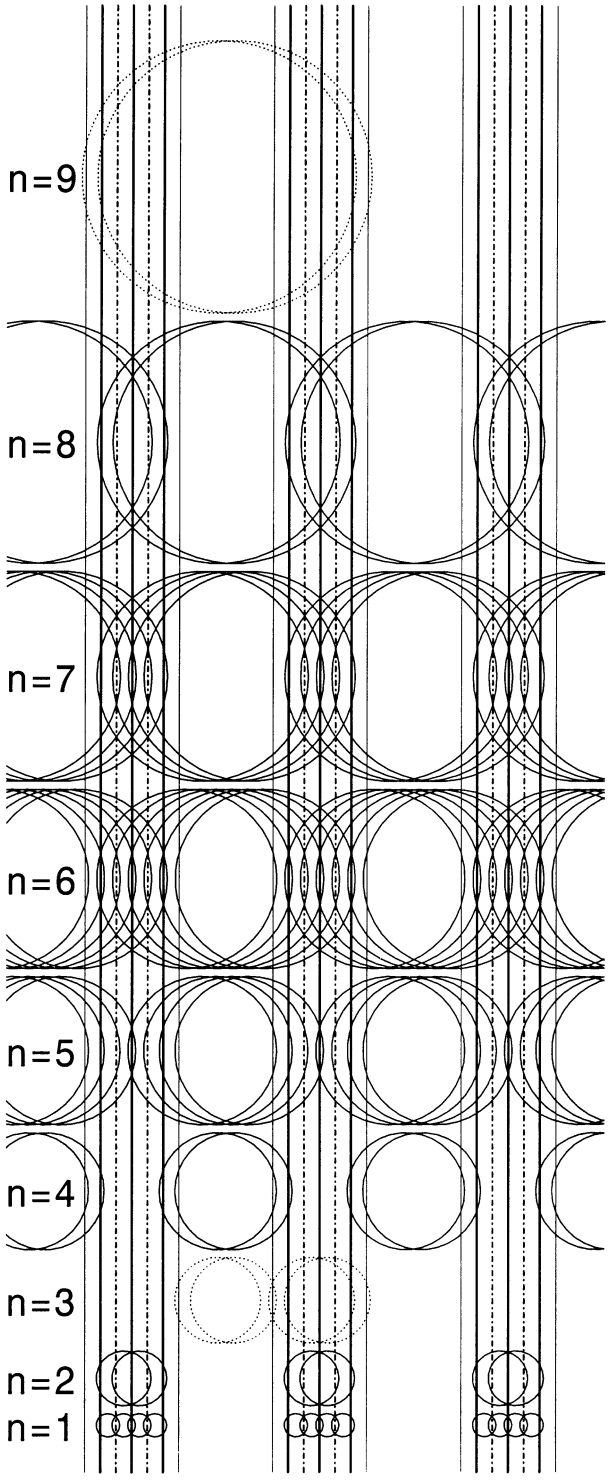

Fig. 4. Cyclotron trajectories that give minima and have a guiding center position $X = (i/2+1/4)a$ with i integers. Thick solid lines represent potential maxima (the position with resist lines on top), and dot-dashed lines potential minima (the position between the resist lines). Thin solid lines are boundaries between LSL and open space regions, outside which modulation electric field is absent (see potential profile in Fig. 1). Dotted trajectories ($n = 3, 9$) are those that cannot contribute to resistivity minima since one of the edges are outside the region where modulation field is present.

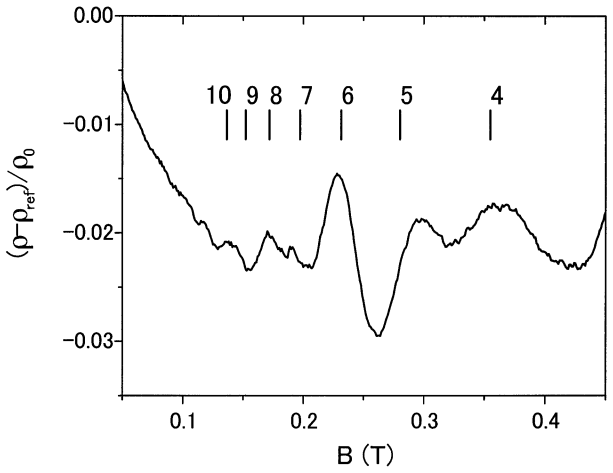

Fig. 5. Magnetoresistance (MR) of a sample with $p = 3$ and $q = 5/2$. Again, short vertical lines indicate positions of minima for ordinary LSL.

and the absence of $n = 4$ dip for $p = q = 4$ can also be explained by similar consideration.

So far we have confined ourselves to the case of q being an integer. The hyperlattice can be, in the case, reproduced by removing from ordinary LSL q periods periodically. We next consider a hyperlattice in a different category; a sample with q being a half odd integer. In Fig. 5, the trace for $p = 3$, $q = 5/2$ is shown. As can be seen, minima appear at the position between those given by eq. (2); actually they occur at position of eq. (3), the position of *maxima* for ordinary LSL. Again this can be explained by considering the classical trajectories. As demonstrated earlier, modulation at the x-minimum and maximum edges of cyclotron trajectory determines the contribution of the trajectory to the MR. Trajectories almost the same at both edges are realized with $2R_c$ that is $a/2$ smaller for this sample compared to the sample in Fig. 2(a). This explains the phase shift by a half period in the minima positions from eq. (2) to eq. (3). An interesting point is that the two elements of the oscillation, the interval and the phase, are controlled independently, the former by a basic period a of the *superlattice* and the latter by the overall period $b = (p + q)a$ of the *hyperlattice*.

To conclude, we have shown that lateral hyperlattice — superlattice of superlattice — shows oscillatory magnetoresistance whose amplitude distribution reflects the number of cyclotron trajectories causing the corresponding oscillation. The phase of the oscillation are shown to be manipulated by the separation between two adjacent "superlattice" regions within a hyperlattice, independently from the interval of extrema, which is determined by the period of the constituting superlattice.

This work was supported in part by Grant-in-Aid for Scientific Research (10740142) from the Ministry of Education, Science, Sports, and Culture, and also in part by a grant from Foundation Advanced Technology Institute.

1) D. Weiss, K. von Klitzing, K. Ploog and G. Weimann: Europhys. Lett. **8** (1989) 179.
2) C. Zhang and R. R. Gerhardts: Phys. Rev. B **41** (1990) 12850.
3) F. M. Peeters and P. Vasilopoulos: Phys. Rev. B **46** (1992) 4667.
4) C. W. Beenakker: Phys. Rev. Lett. **62** (1989) 2020.
5) R. Cuscó, M. C. Holland, J. H. Davies, I. A. Larkin, E. Skuras, A. R. Long and S. P. Beaumont: Surf. Sci. **305** (1994) 643.
6) A. R. Long, E. Skuras, S. Vallis, R. Cuscó, I. A. Larkin, J. H. Davies and M. C. Holland: Phys. Rev. B **60** (1999) 1964.
7) M. Kato, A. Endo and Y. Iye: J. Phys. Soc. Jpn. **66** (1997) 3178.
8) In Fig. 1, potential profile is depicted as if the potential is higher under the resist lines than under the open spaces. This is not at all clear and can be the other way around. However, the sign of the potential does not affect any part of the present argument. Therefore we just tentatively assume this for convenience throughout the present paper.
9) J. Fujita, Y. Ohnishi, Y. Ochiai and S. Matsui: Appl. Phys. Lett. **68** (1996) 1297; J. Fujita, Y. Ohnishi, S. Manako, Y. Ochiai, E. Nomura, T. Sakamoto and S. Matsui: Jpn. J. Appl. Phys. **36** (1997) 7769.
10) E. Skuras, A. R. Long, I. A. Larkin, J. H. Davies and M. C. Holland: Appl. Phys. Lett. **70** (1997) 871.
11) I. A. Larkin, J. H. Davies, A. R. Long and R. Cusco: Phys. Rev. B **56** (1997) 15242.
12) C. J. Emeleus, B. Milton, A. R. Long, J. H. Davies, D. E. Davies, D. E. Petticrew and M. C. Holland: Appl. Phys. Lett. **73** (1998) 1412.
13) Y. Paltiel, D. Mahalu, H. Shtrikman, G. Bunin and U. Meriav: Semincond. Sci. Technol. **12** (1997) 987.
14) A. Endo, S. Katsumoto and Y. Iye: submitted to Phys. Rev. B.